



Influence of Temperature on Capacitance and Dielectric permittivity of Disc-shaped Compact fabricated from Periwinkle Shell Powder

Edidiong Iwok Umanah¹, Nsikak Edet Ekpenyong¹, Aniefiok Otu Akpan¹

Received: October 27, 2022 / Accepted: December 5, 2022

© REJOST 2022

Abstract

Periwinkle shells are often generated in large quantities as waste but still remain under-utilised. Prevalently, they are heaped in open fields and landfills. Such disposal method enhances environmental pollution and breeding of disease-carrying organisms, thereby posing severe adverse effects on public health. This research aimed at devising a way to address the problems while deriving benefits from the approach. Periwinkle shells were gathered, washed, dried, and processed into powdery form which then after was blended with a wetting liquid (of viscosity 9.2×10^{-4} Pas, prepared from dry cassava starch). The blended material was utilised to produce five identical disc-shaped compacts used as test samples in this study. Capacitance of the samples was measured at frequencies of 1 kHz, 10 kHz, and 100 kHz over a temperature range of 20 °C to 70 °C. It was observed that, irrespective of the frequency considered, the samples exhibited negative temperature coefficient of capacitance.

Also, the dielectric permittivity decreased as frequency increased but ranged in values (4.73 – 9.06), (2.16 – 7.02), and (1.86 – 6.33) within the adopted temperatures limits. Again, it was noticed that the samples could serve as a suitable alternative to conventional dielectrics such as paper, mica, aluminium oxide, and glass which are usually and commonly applied for capacitor manufacturing. Hence, valorisation of Periwinkle shells could serve as a scientific way of solving the associated disposal problems while availing electrical/electronic industries with low-cost, environmentally-friendly, and promising dielectric material suitable for use in capacitive energy storage devices. In the alternative, the samples could be used for electrical insulation in systems designed to operate at temperature that exceeds room value by up to 70 °C.

Keywords: Cassava starch; Conventional dielectrics; Hausner ratio; Temperature coefficient; Wastes

✉ Edidiong Iwok Umanah:

edidiongumanah1994@gmail.com

¹Department of Physics, Akwa Ibom State University, Ikot Akpaden, Mkpate Enin, Akwa Ibom State, Nigeria

1.0 Introduction

Periwinkle, commonly known as sea snail, is a typical shell food that is considered a delicacy in most African and Asian cuisines. Its meat is

high in protein, selenium, and magnesium and also rich in Omega-3 fatty acids. Some health benefits derived from consumption of Periwinkle meat include improvement of brain memory, reduction of risk of high blood pressure, cancer, reproductive and heart diseases, as well as synthesis of fats and nucleic acids. According to The Sun Newspaper report dated February 1, 2019, Periwinkle constitutes all the vital vitamins required by human body. This agrees with the observation of Ekop *et al.* (2011) that periwinkle meat presents economic potentials mainly due to its excellent protein quality and availability all year round. Compared to Oyster, Whelk, and Clam, Periwinkle meat has about (70.42 ± 0.030) being the highest protein content (Johnnie *et al.*, 2020). In Nigeria, there are about twelve million tonnes of waste shells disposed of on land and seashores annually (Hart, 2020) and a considerable amount of them are Periwinkle shells (Aimikhe and Lekia, 2021). When the edible part (meat) is removed, the residual solids (Periwinkle shells) are usually discarded as waste materials. According to some reported research findings, these shells can be used for development of asbestos-free automotive brake pad (Yawas *et al.*, 2016), manufacturing of abrasive material (Obot *et al.*, 2017) and as coarse aggregates for production of normal-weight concrete (Eziefula *et al.*, 2020; Omisande *et al.*, 2020; Amarachi *et al.*, 2021). Also, Periwinkle shell powder is a useful pharmaceutical excipient (Ugoeze and Chukwu, 2017) and incorporating it into polypropylene can yield composites with improved wear resistance and fatigue strength (Onuoha, 2019). Anita *et al.* (2020) utilised up to 30 % of Periwinkle shell ash for cement replacement in lateritic soil and observed satisfactory results. At 10 % level of Periwinkle shell ash substitution for cement, increase in splitting tensile strength of concrete is possible (Kolapo and Umoh, 2012). According to Aisien *et al.* (2015), Periwinkle shell ash is a useful

photocatalyst for degradation of aniline in aqueous solution.

However, Periwinkle shells are observed to be under-utilised. This situation warrants heaping them frequently in open fields and landfills. Such prevalent disposal method enhances environmental pollution and breeding of disease-carrying organisms thereby posing severe adverse effects on public health. Since solid waste management system remains inefficient and waste generation increases astronomically with population (Robert *et al.*, 2021), it is necessary to consider other ways of addressing the situation while benefiting from the approach. Hence, the essence of this study is to ascertain the feasibility of utilising Periwinkle shells for dielectric/electrical applications in order to provide a route for solving the above-identified disposal problems. Electrical properties of discs fabricated from Periwinkle shell nanopowder (Adeniran *et al.*, 2022) and those of Periwinkle shell powder filled polymer composites (Abdelmalik and Sadiq, 2019) have been studied and reported. Specifically, disc-shaped compacts fabricated from Periwinkle shell powder will be examined for capacitance and dielectric permittivity as a function of temperature. Interestingly, there is no scientific information in the literature on such consideration for Periwinkle shells. It is therefore hoped that findings from this work would be of immense benefit to researchers, engineers, and electrical/electronic industry.

2.0 Experimental perspective

2.1 Materials

The major materials utilised in this study were cassava effluent and Periwinkle shells. They were obtained as waste materials and in large quantities. Whereas the Periwinkle shells were picked from dumpsites, the cassava effluent was collected from local cassava processing units. Both materials were sourced within

Mkpat Enin Local Government Area, Akwa Ibom State, Nigeria.

2.2 Processing of the waste materials

Prior to their use for development of test samples, the as-collected materials were processed into starting materials as described below:

Using the technique employed by Robert *et al.* (2019), starch was obtained from the cassava effluent. In this case, the cassava effluent was put in a plastic bucket and left to settle for 10 hours before it was decanted to obtain the residue (starch). The starch was then subjected to continuous sun-drying and weighing until it became powdery and its weight also remained constant. The Periwinkle shells were washed thoroughly using clean tap water and then dried

in an electric oven (Model N30C, Genlab). This was necessary in order to ensure that dirt and other forms of impurities were removed from them. By means of Agate mortar and pestle, the dried shells were crushed. Figure 1 shows the shells in dried and crushed forms. The crushed material was screened with the aid of a standard sieve and the quantity of it that passed 250 μm – sieve opening was calcined in Muffle ASCO furnace maintained at 1000 $^{\circ}\text{C}$. After 5 hours, the calcined material was allowed to cool to about 35 $^{\circ}\text{C}$ before it was pulverised using a high-energy ball miller (E_{max} , manufactured by RETSCH, GmbH). This ball-milling machine was operated at 500 rpm for 6 hours and it is capable of reducing the particle size of a material feed from about 5 mm to as fine as less than 80 nm.



Fig. 1: Forms of the periwinkle shells used (a) dried (b) crushed

2.3 Analysis of the processed materials

Both the cassava starch (CST) and Periwinkle shell powder (PSP) were analysed, separately, for flowability on the basis of their Hausner

ratio. Using a digital weighing balance (S. METTLER – 600G), 10 g of each material was weighed and transferred to a 100 cm^3

measuring cylinder. The volume occupied by it at that instant was noted as loose bulk volume. The cylinder was then tapped 100 times and the volume of the material in it was noted as tapped volume. By calculation, the bulk density ρ_b and tapped density ρ_t were determined based on conventional density formula (Etuk *et al.*, 2018, 2020a; Robert *et al.*, 2020; Okorie *et al.*, 2020) thus:

$$\rho = \frac{M}{V} \quad 1$$

where ρ = bulk or tapped density, M = mass of the material, and V = bulk or tapped volume of the material. From the data obtained, the Hausner ratio H_r was computed as (Reddy *et al.*, 2014).

$$H_r = \frac{\rho_t}{\rho_b} \quad 2$$

2.4 Discs (samples) fabrication

The PSP was carefully blended into a wetting liquid (having viscosity of 9.2×10^{-4} Pas) to form homogeneous mixture consisting of six parts of the powder to one part of the liquid by weight. For preparation of the wetting liquid, 10 % solution of the cassava starch was mixed with hot water and the mixture was heated by means of an electric hotplate (Lloytron E4102EH) until it became mildly viscous. Disc-shaped compact of diameter 16.0 mm (as measured by means of digital vernier callipers) was obtained by pressing the resulting homogeneous mixture uniaxially at 7×10^2 MPa. This was allowed for 20 minutes after which the compact was sintered at 1000°C in air for 1 hour before it was diced into five identical samples of thickness 2.0 mm.

2.4 Test protocols

At a time, a sample was engaged in a holder equipped with two lead terminals and a unit for assemblage of a disc-shaped component. For the purpose of capacitance measurement, the lead terminals of the holder were connected to the probes of a calibrated LCR meter (Model

No. 9183, Lutron). A digital thermometer (Model no. 305, calibrated as well and equipped with type $-K$ probe) was employed for temperature monitoring and measurement. The thermometer probe was clamped such that its tip made contact with one cross-section of the sample under test. Figure 2 shows the features of the setup used. The hotplate served as source of heat. The metallic pins holding the sample in the assembly were properly lagged (using cotton wool) to ensure that only the heat absorbed by the sample caused variations in its capacitance values during each test schedule. By adjusting the control dial of the hotplate to a reasonable position, the heat supplied to the system was made to flow slowly through the aluminium block into the sample. As the temperature of the sample increased by 5°C , the capacitance of the sample was noted at three different frequencies. All the samples were similarly tested.

2.5 Properties determination

The mean and standard error values of capacitance were determined for each temperature per frequency. Temperature coefficient of capacitance was deduced graphically based on two standards, namely, Japanese Industrial Standards (JIS) and Electronic Industries Alliance (EIA). In mathematical form,

$$C_t = \left(\frac{C_m - C_r}{C_r \Delta T} \right) 100 \% \quad 3$$

where C_t = temperature coefficient of capacitance, C_r = capacitance value at reference temperature, ΔT = difference between maximum operating temperature and reference temperature values, and C_m = capacitance value at operating temperature. The dielectric permittivity value was obtained for each temperature by applying the relation (Iboh *et al.*, 2020; Etuk *et al.*, 2020b, 2022; Umanah *et al.*, 2022)

$$C = \epsilon_r \epsilon_o \left(\frac{A}{d} \right) \quad 4$$

where C = mean capacitance value per temperature, A = cross-sectional area of the sample, d = thickness of the sample, and ϵ_0 = permittivity of free space ($8.85 \times 10^{-12} \text{ Fm}^{-1}$).

3.0 Results and Discussion

Table 1 shows particulars describing the PSP and CST used to fabricate the samples. Their

mean Hausner ratios are approximately the same. Based on the interpretation given for flowability of materials (Lebrun *et al.*, 2012), it could be adjudged that PSP and CST have good flow characteristics. Thus, they are suitable for manufacturing purpose as utilised in this research.

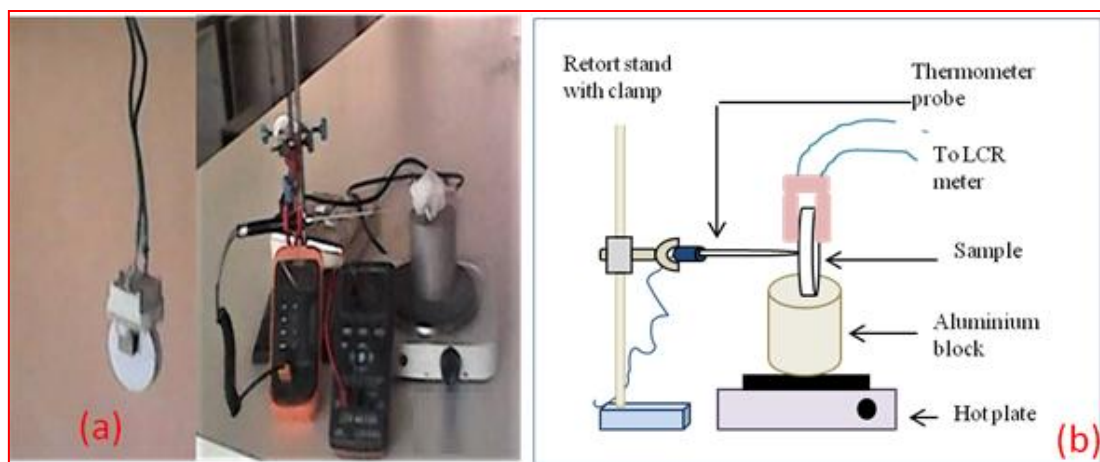


Fig. 2: Setup features (a) Engaged sample (b) Experimental diagram (c) Schematic diagram

Table 1: Particulars of the processed materials

Name	Code	Form	Hausner ratio			
			1	2	3	Mean \pm std. error
Periwinkle shell powder	PSP	Dry	1.13	1.10	1.12	1.12 ± 0.01
Cassava starch	CST	Dry	1.13	1.12	1.14	1.13 ± 0.01

The capacitance – temperature data for the samples at frequencies of 1 kHz, 10 kHz, and 100 kHz are recorded in Table 2. As seen, capacitance varies negatively with frequency at all temperatures. This may be attributed to the fact that the time for dipoles to orient in the applied electric field is less as the frequency progressively increases. The capacitance values at temperatures of 60 °C and 30 °C and frequencies of 1 kHz and 10 kHz, respectively, compare very well. Similar observation is in the case of temperature at 65 °C and 55 °C with frequency of 10 kHz and 100 kHz respectively. Over the range of temperature measurements, the capacitance values of the samples change by about 47.77 %, 69.23 %, and 70.69 % at frequency of 1 kHz, 10 kHz, and 100 kHz

respectively. One-way analysis of variance (ANOVA) performed at $p < 0.05$ using Statistical Package for the Social Sciences (SPSS) software reveals calculated value of 16.16 %, 26.22 %, and 0.77 % between values obtained at 1 kHz and 10 kHz, 1 kHz and 100 kHz, and 10 kHz and 100 kHz respectively. These portray a significant difference except in the case of 0.77 %. In all the cases, figure 3 depicts that capacitance decays non-linearly with increase in temperature of the samples. This signifies that the samples have negative temperature coefficient of capacitance. As frequency increases, the capacitance decreases for each of the temperature values. The nature of curves in this study agrees with the cases involving temperature coefficient of

capacitance of some BaTiO₃-based ceramics at 100 kHz for temperature above 120 °C as noted by Dean *et al.*, (2016). For capacitor

applications, the studied samples can be used to cancel temperature effects on other components in a circuit.

Table 2: Capacitance – temperature data for the samples

Temperature, T (°C)	Measured capacitance, C (10^{-12} F) per frequency, f		
	$f = 1.0$ kHz	$f = 10.0$ kHz	$f = 100.0$ kHz
20.0	8.06 ± 0.04	6.24 ± 0.03	5.63 ± 0.02
25.0	7.48 ± 0.03	5.51 ± 0.02	4.85 ± 0.02
30.0	7.04 ± 0.02	4.82 ± 0.02	4.31 ± 0.02
35.0	6.51 ± 0.03	4.13 ± 0.02	3.53 ± 0.01
40.0	6.30 ± 0.02	3.72 ± 0.03	3.15 ± 0.02
45.0	5.82 ± 0.02	3.51 ± 0.03	2.57 ± 0.02
50.0	5.44 ± 0.02	2.85 ± 0.02	2.34 ± 0.02
55.0	5.10 ± 0.03	2.53 ± 0.02	2.07 ± 0.01
60.0	4.83 ± 0.02	2.31 ± 0.02	1.96 ± 0.02
65.0	4.44 ± 0.01	2.05 ± 0.02	1.75 ± 0.01
70.0	4.21 ± 0.01	1.92 ± 0.01	1.65 ± 0.01

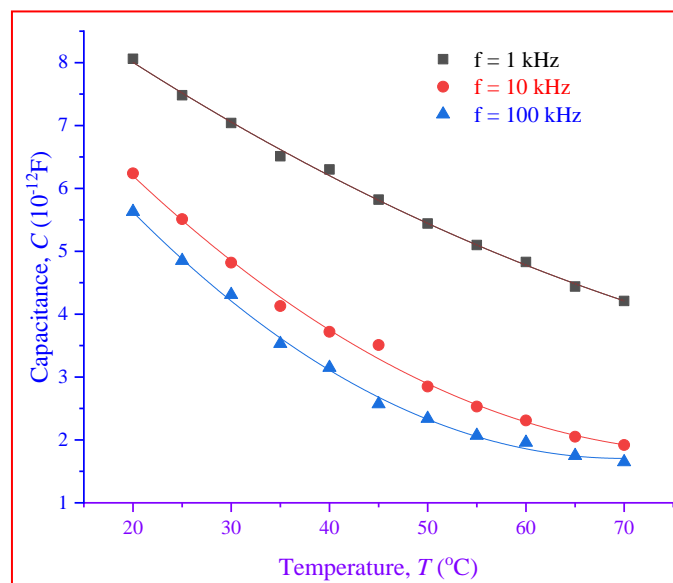


Fig. 3: Variation of capacitance with temperature of the samples

Table 3 shows the temperature coefficients of capacitance obtained for the samples in accordance with both the JIS and EIA standards. With respect to the reference temperature for each standard, the fractional change in the values of each sample's capacitance over the resulting temperature range correlates positively with frequency. It appears from the results that, if used as a dielectric for capacitor making, realisation of

very satisfactory performance would be possible within audio frequency range. Regarding dielectric permittivity of the samples, as presented in Table 4, the values obtained at 1 kHz from at least 40 °C tend to compare with values obtained at 10 kHz and 100 kHz from 20 °C to 35 °C and 30 °C respectively. This means that under such conditions of operation, the samples are capable of exhibiting similar operational tendencies in

an applied electric field as long as storage of electric charges is concerned. For the limits of temperature values considered, the range (4.73 – 9.06), (2.16 – 7.02), and (1.86 – 6.33) in values of the dielectric permittivity are obtained for the samples at 1 kHz, 10 kHz, and 100 kHz respectively. As frequency increases, the dielectric permittivity decreases, a similar observation reported by Rahmoouni et al. (2015). Schultz (2011) reported the dielectric permittivity values of some conventional dielectrics such as paper (2 - 6), mica (3 – 8), aluminium oxide (7), and glass (8) commonly utilised for capacitor making. Comparatively, it could be remarked that the samples are suitable alternative dielectrics to paper for use from 20 °C to 70 °C at frequencies between 1 kHz and 100 kHz. Also, it is not inappropriate to submit that the performance of the samples at 1 kHz (between 25 °C and 70 °C), 10 kHz (from 20 °C to 60 °C), and 100 kHz (between 20 °C and 50 °C) could compare very well with that of mica. However, at 1 kHz, the samples have the highest dielectric permittivity value (9.06) compared to the above-named conventional dielectrics. Since insulating materials that have high dielectric permittivity values are suitable candidates for capacitor manufacturing, it can be averred that the samples are promising alternatives for fabrication of energy storage devices like capacitors. This resonates with the submission of Halizan *et al.* (2021) that good dielectric permittivity material has huge potential in capacitive energy storage devices for electronic applications. More so, Etuk *et al.* (2020b) reported dielectric permittivity values of 2.632 at 1 kHz and 4.196 at 10 kHz for membranes of Quail egg and Duck egg respectively. These are not significantly different from the respective values of 2.63 and 4.18 obtained for the samples at 100 kHz (and 50 °C) and 10 kHz (and 40 °C). For the samples, the highest dielectric permittivity value is 7.02 at 10 kHz and 6.33 at 100 kHz.

Though these values are greater by 26.03 % and 73.90 %, respectively, than those reported by Etuk *et al.* (2022) at same frequencies for fibre of young epidermis of *raphia vinifera* at room temperature, the maximum value of 9.06 obtained for the samples at 1 kHz is less by 18.67 % than the one obtained for the said fibre.

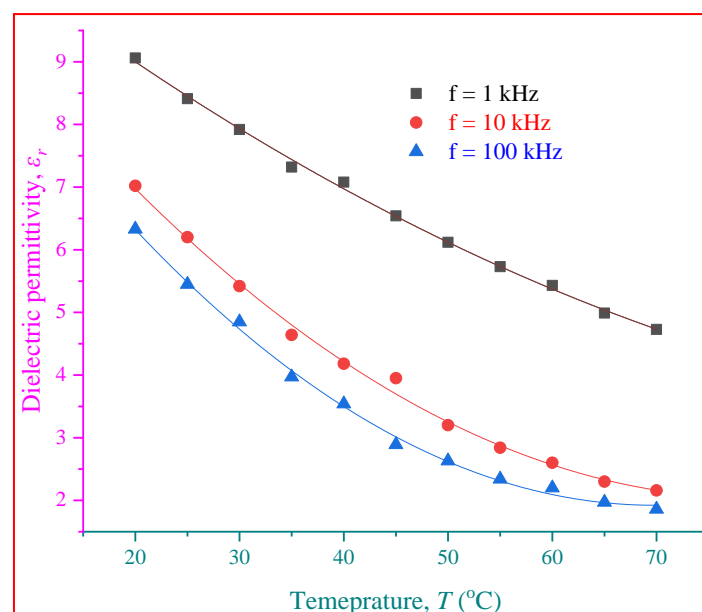
From figure 4, it is obvious that dielectric permittivity of the samples trends inversely and in a non-linear manner with increasing temperature. The remarkable variation noticed in the trend signifies that the samples possess permanent dipoles and is due to the effect of heat on orientation polarisation. Explaining in other words, the amount of polarisation could be understood as the degree of perfect alignment of molecules of a dielectric material with an external electric field. Now, the more aligned the molecules are with the field, the more is the polarisation and hence, the dielectric permittivity. But with increase in temperature, there is increase in thermal agitation of the molecules which results to more randomness in their alignment with the field. This equally reduces polarisation and in turn, dielectric permittivity. The inverse relationship in dielectric permittivity with temperature is in agreement with the findings of Bahr et al. (2011) in the case of Tl_2S layered single crystals. It also supports the report of Lee et al. (2006) on temperature coefficient of capacitance of nanocomposites. Since the samples are insulating and their dielectric permittivity diminishes as temperature increases above room value, they could be applied for electrical insulation in systems designed to operate at such high temperature levels. Considering that practical capacitors are often constructed by means of high permittivity dielectrics (Brindley and Carr, 2002), the samples can give satisfactory performances if used as a dielectric for capacitor production.

Table 3: Temperature coefficient of capacitance of the samples

Frequency, f (kHz)	C_t (%/°C) per standard	
	JIS	EIA
1.0	- 0.96	- 0.97
10.0	- 1.38	- 1.48
100.0	- 1.41	- 1.47

Table 4: Dielectric permittivity of the samples at various temperatures

Temperature, T (°C)	Mean dielectric permittivity, ϵ_r per frequency		
	$f = 1.0$ kHz	$f = 10.0$ kHz	$f = 100.0$ kHz
20.0	9.06	7.02	6.33
25.0	8.41	6.20	5.45
30.0	7.92	5.42	4.85
35.0	7.32	4.64	3.97
40.0	7.08	4.18	3.54
45.0	6.54	3.95	2.89
50.0	6.12	3.20	2.63
55.0	5.73	2.84	2.34
60.0	5.43	2.60	2.20
65.0	4.99	2.30	1.97
70.0	4.73	2.16	1.86

**Fig. 4** Variation of dielectric permittivity with temperature of the sample

4.0 Conclusion

The results of measurements performed in this research showed decrease in capacitance with temperature of disc-shaped compact fabricated from Periwinkle shell powder and cassava starch. At frequency of 1 kHz, 10 kHz, and 100 kHz the respective temperature coefficients of

capacitance obtained (in %/°C) for the sample were found to be - 0.96, - 1.38, and - 1.41 (based on Japanese Industrial Standard) and - 0.97, - 1.48, and - 1.47 (in accordance with Electronic Industries Alliance). The values of dielectric permittivity of the sample compared with those reported in the literature for

conventional dielectric materials like paper, mica, aluminium oxide, and glass commonly used for capacitor manufacturing. Thus, in addition to serving as a route for solving disposal problems, recycling cassava effluent into starch and Periwinkle shells into powdery form and then utilising them to fabricate the disc as described in this work could help to ensure availability of cost-effective and useful dielectric for capacitor applications.

Conflict of interest

The authors declare that they have no known competing financial interests or personal relationships that could have appeared to influence the work reported in this paper.

Acknowledgements

Not applicable

References

- Abdelmalik, A.A., Sadiq, A., (2019). Thermal and electrical characterization of composite metal oxides particles from periwinkle shell for dielectric application. *SN Applied Sciences*, 1(4); 373, <https://doi.org/10.1007/s42452-019-0388-5>
- Adeniran, A.O., Akankpo, A.O., Etuk, S.E., Robert, U.W., Agbasi. O.E., (2022). Comparative study of electrical resistance of disc-shaped compacts fabricated using calcined clams shell, Periwinkle shell and Oyster shell nanopowder. *Kragujevac J. Sci.* 44; 25–36, <https://doi.org/10.5937/KgJSci2244025A>
- Aimikhe, V.J., Lekia, G.B., (2021). An overview of the applications of Periwinkle (*Tympanotons fascatus*) shells. *Current Journal of Applied Science and Technology*, 40(18); 31 – 58, <https://doi.org/10.9734/CJAST/2021/v40i1831442>
- Aisien, F., Amenaghawon, A.N., Oshomogho, F., (2015). Application of Periwinkle shell ash as photocatalyst in the heterogeneous photocatalytic degradation of aniline in aqueous solution. *Journal of Materials and Environmental Science*, 6(2), 572 – 579
- Anita, M. E., Ajero, I.K., Anih, P.C., (2020). The Effect of Periwinkle shell ash mixed with cement on water absorption and shrinkage of lateritic block. *Baltic Journal of Real Estate Economics and Construction Management*, 8(1), 22 – 33, <https://doi.org/10.2478/bjreecm-2020-0003>
- Amarachi, N., Gerald, O., Emeka, O., Martin, O., (2021). The Future and Prospects of Periwinkle Composites in Reinforced Concretes: A Review. *Journal of Engineering Research and Reports*, 21(1): 49-67, <https://doi.org/10.9734/JERR/-2021/v21i117439>
- Badr, A.M., Elshaikh, H.A., Ashraf, I.M., (2011). Impacts of Temperature and Frequency on the Dielectric Properties for insight into the Nature of the Charge Transports in the Tl_2S layered single crystals. *Journal of Modern Physics*, 2(1), Article ID 3764, <https://doi.org/10.4236/jmp.2011.21004>
- Brindley, K., Carr, J., (2002). *Newnes Electronics Engineer's Pocket Book*, 2nd edn., Reed Educational and Professional Publishing Ltd., Johannesburg Melbourne, New Delhi, p. 13, ISBN 0750639725
- Dean, J. S., Foeller, P.Y., Reaney, I.M., Sinclair, D.C., (2016). A resource efficient design strategy to optimise the temperature coefficient of capacitance of BaTiO₃-based ceramics using finite element modelling. *Journal of Materials Chemistry A*, 4; 6896 – 6901, <https://doi.org/10.1039/c5ta09573e>
- Ekop, I. E., Simonyan, K.J., Onwuka, U.N., (2021). Effects of processing factors and conditions on the cracking efficacy of *Tympanotonus fuscatus* and *Pachymelania aurita* periwinkles:

- Response Surface Approach. *Journal of Agriculture and Food Research*, 3(11), 100094, <https://doi.org/10.1016/j.jafr.2020.100094>
- Etuk, S.E., Agbasi, O.E., Abdulrazzaq, Z.T., Robert, U.W., (2018). Investigation of thermophysical properties of Alates (swarmers) termites wing as potential raw material for insulation. *Int. J. Sci. World*, 6(1), 1 – 7, <https://doi.org/10.14419/ijsw.v6i1.8529>
- Etuk, S.E., Agbasi, O.E., Ekpo, S.S., Robert, U.W., (2020a). Gamma Radiation determination of absorption coefficients of cement sand block. *Cumhuriyet Science Journal*, 41(1), 38 – 42, <https://dx.doi.org/10.177776/csj.624318>
- Etuk, S.E., Robert, U.W., Emah, J.B., Agbasi, O.E., (2020b). Dielectric properties of eggshell membrane of some select bird species. *Arabian Journal for Science and Engineering*, 46(1), 769 – 779, <https://doi.org/10.1007/s13369-020-04931-7>
- Etuk, S.E., Ekpo, S.S., Robert, U.W., Agbasi, O.E., Effiong, E.A., (2022). Dielectric properties of *Raphia fiber* from Epidermis of young *Raphia vinifera* leaflet. *Acta Technica Jaurinensis*, 15(2), 91 – 98, <https://doi.org/10.14513/actatechjaur.00648>
- Eziefula, U.G., Obiechefu, G.C., Charles, M.E., (2020). Use of Periwinkle shell by-products and Portland cement-based materials: an overview. *Intl J Environment and Waste Management*, 26(3), 362 – 388, <https://doi.org/10.1504/IJEW.2020.109165>
- Halizan, M.Z.M., Mohamed, Z., Yahya, A.K., (2021). Understanding the structural, optical, and dielectric characteristics of SrLaLiTe_{1-x}Mn_xO₆ perovskites. *Scientific Reports*, 11; 9744, <https://doi.org/10.1038/s41598-021-89132-4>
- Hart, A., (2020). Mini-review of waste shell-derived materials applications. *Waste Management and Research*, 38(5); 514 – 527
- Iboh, U.A., Robert, U.W., Umoren, G.P., Okorie, U.S., (2020). The effect of frequency variation on dielectric constant of *raphia hookerie*. *Journal of Renewable Energy and Mechanics*, 3(2), 53 – 58, [https://doi.org/10.25299/rem.2020.vol3\(02\).4433](https://doi.org/10.25299/rem.2020.vol3(02).4433)
- Johnnie, E.O., Chituru, A.S., Barine, K.K.D., Joy, E., (2020). Determination of Protein Quality of Oven-dried Clam (*Mecmermeria in*), Whelk (*Thias c*), Oyster (*Crossostrea g.*) and Periwinkle (*Tympanotonus f.*) meat using rat Bioassay. *American Journal of Food Science and Technology*, 8(5), 172 – 175, <https://doi.org/10.12691/ajfst-8-5-1>
- Kolapo, O., Umoh, A.A., (2012). Strength characteristics of Periwinkle shell ash blended cement concrete. *International journal of architecture Engineering and Construction*, 1(4), 213 – 220, <https://doi.org/10.7492/IJAEC.2012.023>
- Lebrun, P., Krier, F., Mantanus, J., Grohganz, H., Yang, M., Rozet, E., Boulanger, B., Evrard, B., Rantanen, J., Hubert, P., (2012). Design space approach in the optimization of the spray-drying process. *Eur. J.Pharm. Biopharm.* 80; 226–234
- Lee, B., Abothu, I.R., Raj, P.M., Yoon, C.K., Tummala, R.R., (2006). Tailoring of temperature coefficient of capacitance (TCC) in nanocomposite capacitors. *Scripta Materialia*, 54; 1231–1234, <https://doi.org/10.1016/j.scriptamat.2005.12.026>
- Obot, M.U., Yawas, D.S., Aku, S.Y., (2017). Development of an abrasive material using Periwinkle shells. *Journal of King Saud University – Engineering Sciences*, 29(3), 284 – 288, <https://doi.org/10.1016/j.jksues.2015.10.008>

- Okorie, U.S., Robert, U.W., Iboh, U.A., Umoren, G.P., (2020). Assessment of the suitability of tiger nut fibre for structural applications. *Journal of Renewable Energy and Mechanics*, 3(1); 32 – 38, [https://doi.org/10.25299/rem.2020.vol3\(01\).4417](https://doi.org/10.25299/rem.2020.vol3(01).4417)
- Omisande, L. A., Onugba, M. A., (2020). “Sustainable Concrete Using Periwinkle Shell as Coarse Aggregate – A Review.” *IOSR Journal of Mechanical and Civil Engineering (IOSR-JMCE)*, 17(6); 17 – 22, <https://doi.org/10.9790/1684-1706031722>
- Onuoha, C., (2019). Tribological Behaviour of Periwinkle Shell Powder – filled Recycled Polypropylene Composites. *International Journal of Engineering and Technologies*, 17, 11 – 20, <https://doi.org/10.18052/www.scipress.com/IJET.17.11>
- Rahmouni, H., Smari, M., Cherif, B., Dhahri, E., Khirouni, K., (2015). Conduction mechanism, impedance spectroscopic investigation and dielectric behavior of $\text{La}_{0.5}\text{Ca}_{0.5-x}\text{Ag}_x\text{MnO}_3$ manganites with the composition below the concentration limit of silver solubility in perovskites ($0 \leq x \leq 0.2$). *Dalton Transactions*, 44; 10457 – 10466, <https://doi.org/10.1039/C5DT00444F>
- Reddy, R.S., Ramachandra, C.T., Hiregoudar, S., Nidoni, U., Ram, J., Kammar, M., (2014). Influence of processing conditions on functional and reconstitution properties of milk powder made from Osmanabadi goat milk by spray drying. *Small Ruminant Research*, 119; 130–137, <http://dx.doi.org/10.1016/j.smallrumres.2014.01.013>
- Robert, U.W., Etuk, S.E., Umoren, G.P., Agbasi, O.E., (2019). Assessment of thermal and mechanical properties of composite board produced from coconut (*Cocos nucifera*) husks, waste newspapers, and cassava starch. *Intl J Thermophys*, 40 (9); 83, <https://doi.org/10.1007/s10765-019-2547-8>
- Robert, U.W., Etuk, S.E., Agbasi, O.E., Umoren, G.P., (2020). Comparison of clay soils of different colors existing under same conditions in a location. *Imam Journal of Applied Sciences*, 5(2), 68 – 73, https://doi.org/10.4103/ijas_35_19
- Robert, U.W., Etuk, S.E., Agbasi, O.E., Ekong, S.A., Abdulrazzaq, Z.T., Anonaba, A.U., (2021). Investigation of Thermal and Strength Properties of Composite Panels Fabricated with Plaster of Paris for Insulation in Buildings. *Intl J Thermophys.*, 42(2) 1 -18, <https://doi.org/10.1007/s10765-020-02780-y>
- Schultz, M.E., (2011). *Grob’s Basic Electronics*, 11th edn., McGraw-Hill Companies, New York, pp.478, ISBN 978-0-07-122137-5
- Ugoeze, K.C., Chukwu, A., (2017). Physico-chemical properties of a modified biomaterial from *Tympanotonus fuscata* (periwinkle) shell powder considered as pharmaceutical excipient. *Journal of Pharmaceutical and Allied sciences*, 14(1), 2417 – 2429
- Umanah, E.I., Ekpenyong, N.E., Akpan, A.O., (2022). Electrical and dielectric properties of discs fabricated using Periwinkle shell nanopowder and dry cassava starch. *Bulletin of the Polytechnic Institute of Iași*, 68(72); 1, 7-20, <https://doi.org/10.2478/bipmf-2022-0001>
- Yawas, D.S., Aku, S.Y., Amaren, S.G., (2016). Morphology and Properties of periwinkle shell asbestos-free brake pad. *Journal of King Saud University - Engineering Sciences*, 28(1), 103 – 109, <http://dx.doi.org/10.1016/j.jksues.2013.11.002>